Journal of Alzheimer's Disease 37 (2013) 551–563
DOI 10.3233/JAD-130602
IOS Press

Research Report

Hyperphosphorylation Results in Tau Dysfunction in DNA Folding and Protection

Yang Lu[a,b], Hai-Jin He[a], Jun Zhou[a,d], Jun-Ye Miao[a,d], Jing Lu[a], Ying-Ge He[a], Rong Pan[a], Yan Wei[a,*], Ying Liu[a] and Rong-Qiao He[a,c,*]

[a]*State Key Laboratory of Brain and Cognitive Sciences, Institute of Biophysics, Chinese Academy of Sciences, Beijing, China*

[b]*School of Life Science, University of Science and Technology of China, Anhui, China*

[c]*Key Laboratory of Mental Health, Institute of Psychology, Chinese Academy of Sciences, Beijing, China*

[d]*University of Chinese Academy of Sciences, Beijing, China*

Accepted 15 July 2013

Abstract. Hyperphosphorylation of tau occurs in preclinical and clinical stages of Alzheimer's disease (AD), and hyperphosphorylated tau is the main constituent of the paired helical filaments in the brains of mild cognitive impairment and AD patients. While most of the work described so far focused on the relationship between hyperphosphorylation of tau and microtubule disassembly as well as axonal transport impairments, both phenomena ultimately leading to cell death, little work has been done to study the correlation between tau hyperphosphorylation and DNA damage. As we showed in this study, tau hyperphosphorylation and DNA damage co-occurred under formaldehyde treatment in N2a cells, indicating that phosphorylated tau (*p*-Tau) induced by formaldehyde may be involved in DNA impairment. After phosphorylation, the effect of tau in preventing DNA from thermal denaturation was diminished, its ability to accelerate DNA renaturation was lost, and its function in protecting DNA from reactive oxygen species (ROS) attack was impaired. Thus, *p*-Tau is not only associated with the disassembly of the microtubule system, but also plays a crucial role in DNA impairment. Hyperphosphorylation-mediated dysfunction of tau protein in prevention of DNA structure from damage under the attack of ROS may provide novel insights into the mechanisms underlying tauopathies.

Keywords: Alzheimer's disease, DNA protection, formaldehyde, GSK-3β, phosphorylation, tau hyperphosphorylation, tau protein, tauopathy

INTRODUCTION

Tau was originally identified as a protein promoting the assembly of microtubules and maintaining microtubules. It is expressed mainly in the axonal compartment of neurons [1], where it also functions in stabilizing and protecting DNA double-strands [2–9]. Its activity is regulated by phosphorylation [10–12], which is reflected in the fact that its primary sequence contains an unusual high number of potential phosphorylation sites [13, 14]. Upon posttranslational modification by phosphorylation, a process of dissociation of tau from microtubules is initiated, resulting in microtubule disassembly and subsequent impairment of axonal transport [15–17]. Hyperphosphorylated tau is the main constituent of paired helical filaments

*Correspondence to: Rong-Qiao He, State Key Laboratory of Brain and Cognitive Sciences, Institute of Biophysics, Chinese Academy of Sciences, 15 Datun Road, Chaoyang District, Beijing 100101, China. Tel.: +86 10 64889876; Fax: +86 10 64875055; E-mail: herq@sun5.ibp.ac.cn.; Yan Wei, State Key Laboratory of Brain and Cognitive Sciences, Institute of Biophysics, Chinese Academy of Sciences, 15 Datun Road, Chaoyang District, Beijing 100101, China. Tel.: +86 10 64888531; Fax: +86 10 64875055; E-mail: yanwei@moon.ibp.ac.cn.

ISSN 1387-2877/13/$27.50

[18, 19], which are structures associated with the development of mild cognitive impairment and Alzheimer's disease (AD) [20–22]. Hyperphosphorylated tau has also been identified in other tauopathies, a class of neurodegenerative diseases associated with the pathological aggregation of hyperphosphorylated tau in the brain [3, 23, 24]. Apart from the axon and cytoplasm [25], hyperphosphorylated tau has been detected in the nucleus of neurons as well [26, 27]. However, whether hyperphosphorylation disables tau in its capacity to protect DNA from structural damage has so far eluded investigation.

In most cases, age-related cognitive impairment progresses from a preclinical stage toward a clinical stage [28]. Recently, the focus of AD research shifted toward preclinical molecular events [29], investigating the mechanisms that activate tau kinases and trigger hyperphosphorylation of tau in neurons. Recent work from our group indicated that in N2a cells and mouse brain cells [30], tau is converted to phosphorylated tau (*p*-Tau) upon exposure to formaldehyde, a process that occurs concomitantly with activation of glycogen synthase kinase-3β (GSK-3β), a well-documented tau kinase [16, 31–34]. Furthermore, internally produced formaldehyde is found to correlate positively with human aging as well as with the severity of cognitive impairments in patients with age-related dementia [35, 36]. In addition, it was shown that extracellular formaldehyde, even at a near-physiological concentration induces tau misfolding and subsequent cytotoxicity *in vitro* [37–40]. Rats injected intraperitoneally with 0.5 mM formaldehyde (60 mg/kg) show cognitive deficits in a Morris water maze test, suffering from both acute and chronic signs of impairment of long term potential [41]. However, the relationship between hyperphosphorylation of tau protein induced by physiological concentrations of formaldehyde and DNA damage remains unclear. Investigations were also carried out to clarify whether hyperphosphorylation reduces the ability of tau to associate with DNA, and to protect it from formaldehyde-induced damage.

GSK-3β is shown to be one of the major kinases that phosphorylate specific tau epitopes, such as Thr181 (T181) and Ser396 (S396) [42–44]. Extracellular detection in the cerebrospinal fluid of T181-phosphorylated tau serves as a biomarker for AD prediction [45–47]. Phosphorylation of S396 results in decreased tau solubility *in vitro*, and is believed to be a crucial step in the development of neurofibrillary pathology in AD [48, 49]. Our previous work in N2a cells as well as mouse brain cells showed that both exogenous and endogenous formaldehyde can trigger tau hyperphosphorylation. Here, GSK-3β was employed to convert purified tau into *p*-Tau, and to investigate the effects of tau phosphorylation on tau-mediated DNA folding and protection from thermal denaturation and reactive oxygen species (ROS) attack.

In this study, we aimed to investigate the interaction between *p*-Tau and DNA, in order to clarify how phosphorylation renders tau unable to perform the task of protecting DNA from thermal denaturation and ROS attack. We evaluated the effects of *p*-Tau on DNA folding, which is relevant to the function in protection of DNA. Our findings suggest that tau protein plays a role in DNA folding, possibly by assisting the formation of a structure that protects DNA from an attack by ROS.

MATERIALS AND METHODS

Materials

The following antibodies were used for western blotting and/or immunostaining. Anti-tau (Tau5, a monoclonal antibody recognizing both phosphorylated and non-phosphorylated tau) and anti-pS396 (clone PHF13) were from Millipore (USA); anti-pT181 was from SAB (USA); anti-GSK-3β was from CST (USA). Horseradish peroxidase-conjugated/TRITC-labeled goat anti-mouse/rabbit secondary antibodies were from Zhongshan Goldbridge Biotechnology (China). Formaldehyde and calf thymus DNA were from Sigma (USA). The APO-BrdU™ TUNEL Assay kit was from Invitrogen (USA). All other reagents were of analytic grade and were used without additional purification.

The prokaryotic expression vector Prk172 containing the tau_{352} insert, which is the tau isoform of the lowest molecular weight, courtesy of Dr. Goedert (Medical Research Council, Molecular Biology Unit, Cambridge, UK). Tau_{352} was purified in step-wise with Q-Sepharose, SP-Sepharose, and Sephadex-G75 columns. Protein concentration was determined by BCA assay (Pierce Biotechnology, Rockford). The purity of the protein was assessed by 12% SDS-PAGE electrophoresis. After purification, tau protein showed a single band in the SDS-PAGE (Supplementary Fig. 1a).

Preparation of phosphorylated tau protein

Five μg of tau protein were incubated overnight at 30°C with 5000 U of GSK-3, in a buffer containing 20 mM Tris-HCl (pH 7.5), 10 mM $MgCl_2$, 5 mM DTT, and 2 mM ATP. Phosphorylation of tau was performed

according to the manufacturer's instructions (Sigma, USA). Successful phosphorylation of tau was verified by western blotting with anti-pS396 and anti-pT181 antibodies (Supplementary Fig. 1b).

Animals

Sprague Dawley (SD) rats were from Vital River Laboratories Technology Co., Ltd. (China). All rats were maintained in animal facilities under pathogen-free conditions. All animal experiments were carried out in accordance with the National Institutes of Health Guide for the Care and Use of Laboratory Animals, and were approved by the Biological Research Ethics Committee, Institute of Biophysics, Chinese Academy of Sciences (approval ID SYXK (SPF) 2007-141).

Electrophoretic mobility-shift assay (EMSA)

A 26 bp oligomer (5′actccgtgcataaataataggcactcg3′; 3′gaggcacgtatttattatccgtgagcc5′) was synthesized (Shanghai Sangon Co., China) based on the mouse N-Oct-3 sequence [50]. For effective annealing, one additional nucleotide was added at each 5′ terminus [51]. The polynucleotides were denatured by heating for 5 min to 95°C in a water bath, and the complementary strands were then annealed by cooling down slowly to room temperature. The concentration of the annealed double-stranded DNA (dsDNA) (26 bp) was determined according to the absorbance at 260 nm on a Hitachi U-2010 UV Spectrophotometer (Japan). Tau protein was incubated with 100 ng dsDNA at the ratio [Tau]/[DNA] = 4/1 in 10 μl TNME solution with 20 mM Tris buffer (pH 7.2), 50 mM NaCl, 0.5 mM DTT, 1 mM $MgCl_2$ and 0.5 mM EDTA (RT, 20 min). The quantitative ratio of [Tau]/[DNA] was defined as the ratio of the number of protein molecules to the number of DNA base pairs, unless otherwise stated. The dsDNA-tau complexes were resolved by non-denaturing 20% polyacrylamide gel and run at 100 V in 1 × TBE running buffer (89 mM Tris base, 89 mM boric acid and 2 mM EDTA, pH 8.3) at 4°C for 2 h. Subsequently the gel was stained with EB (0.5 mg/ml) for 30 min and visualized using a gel UVP Image store 7500 system (Dingyong Co., China). Phosphorylated tau and formaldehyde-treated tau (FA-Tau) were subjected to the same procedure. BSA and histone H1 were used as negative and positive control for DNA binding ability, respectively.

To test the effect of formaldehyde on DNA damage, DNA (1 μg of vector Prk172 bearing tau_{352}) incubated with formaldehyde at different concentrations (0, 0.05, 0.1, 0.3, and 1 mM, 37°C, 30 min) was loaded onto a 2% agarose gel. DNA incubated with DNase I for 1 min and 30 min was used as a positive control.

Cell culture, treatments, and cell viability assays

The human (SH-SY5Y) and mouse neuroblastoma (N2a) cell lines were obtained from the Institute of Basic Medical Sciences (Chinese Academy of Medical Sciences, School of Basic Medicine, Peking Union Medical College). Cells were maintained in Dulbecco's Modified Eagle's Medium (DMEM, Invitrogen, USA) supplemented with 10% fetal bovine serum (FBS, PAA, Austria) and then passaged every 3 days when they reached 90% confluency, according to a previously published method [52].

Cells were seeded onto 96-well plates at a concentration of 3×10^5 cells/ml (200 μl). After cell attachment to the plate (24 h), the medium was replaced with fresh DMEM containing 0.3 mM formaldehyde. Cellular morphology was observed under a laser scanning confocal microscope (LSCMFV500, Olympus, Japan) and cell viability was measured using a Cell Counting Kit (CCK-8, Dojindo Molecular Technologies, Japan), according to the manufacturer's instructions [53, 54]. Cells not treated with formaldehyde were used as controls.

DNA damage and cell apoptosis were detected by using the APO-BrdU™ TUNEL Assay according to the manufacturer's instructions [55]. Cells attached to plastic dishes were harvested using 0.25% trypsin and resuspended in cold PBS. Cell suspensions were then fixed with paraformaldehyde for 15 min. After centrifugation (300 × g, 5 min), the supernatant was discarded and the cells were resuspended in 50 μl freshly prepared DNA-labeling solution and incubated overnight at 37°C. After incubation, 1 ml rinse buffer was added to each tube and the samples were centrifuged (300 × g, 5 min) to remove the supernatants. The cell pellets were resuspended and incubated in antibody staining solution in the dark for 30 min. Finally, the cells were transferred onto slides for microscopy analysis. 0.5 ml of propidium iodide/RNase I staining buffer was used to incubate the slides for another 30 min in the dark. Photographs were taken using a FV1000 confocal microscope (Olympus, Japan).

Immunofluorescent staining

Cells were seeded onto a 24-well plate, with each well containing a glass coverslip coated with cell

adhesive. After 24 h of growth, 0.2 mM formaldehyde was added to the N2a cells for a further 4 h. Cells were fixed with 4% paraformaldehyde for 10 min, washed three times with PBS, before being permeabilized with 0.1% TritonX-100/PBS for another 10 min. Following several wash steps, cells were blocked with 10% goat serum/PBS at room temperature for 1 h. Antibodies (anti-pT181, anti-pS396, Tau5, each diluted to 1 : 100 in PBS) together with phalloidin and Hoechst-33258 were added to the cells for overnight incubation at 4°C. After been washed with PBS, slides were incubated with TRITC-labeled goat anti-rabbit/mouse secondary antibodies (1 : 200) for 1 h. Cells were washed with PBS and mounted with 90% glycerol, before sealing the coverslips with nail polish. Immunofluorescence was analyzed by confocal microscopy.

Thermal denaturation and renaturation of DNA in the presence of p-Tau

For kinetic measurements of calf thymus DNA (40 μg/ml) denaturation, a cuvette was incubated with protein ([DNA]/[protein] = 1) in an ultraviolet spectrophotometer and the temperature was kept at 80°C by using a thermal bath. When a sample was added into the cuvette, the absorbance at 260 nm was immediately measured for 20 min. All data were analyzed as described previously [56]. For kinetic measurements of DNA renaturation, samples were incubated for 20 min at 100°C. The absorbance at 260 nm was recorded for 20 min, following the addition of the sample into the cuvette at room temperature. All the data were analyzed as described previously [56].

Isolation of nuclei and chromatin

A Cytoplasmic and Nuclear Protein Extraction Kit (Fermentas, Canada) was used to isolate nuclei from SD rat livers, and the experimental procedures were followed per manufacturer's instructions [57]. The following isolation steps were all performed on ice. Five g of fresh rat liver was rinsed with ice cold PBS (pH 7.3) and blotted dry. Next, liver samples were homogenized gently in PBS and non-homogenized tissue was filtrated through gauze filter. The homogenate was centrifuged (250 × g, 5 min) and the supernatant was removed. 500 μl cell lysis buffer was added into the 100 mg tissue and was kept for 10 min. The cytoplasmic fraction was separated from the nuclear pellet by centrifugation (500 × g, 7 min) and removed within the supernatant. Nuclear pellets were washed using nuclei washing buffer and centrifuged (500 × g, 7 min) before removing the supernatant. The nuclear pellets were then resuspended in 150 μl nuclei storage buffer, and kept on ice prior to analysis.

The chromatin was isolated from nuclei that were incubated with micrococcal nuclease to digest the DNA into nucleosomal fractions as described by Noll and coworkers [58]. One ml of nuclei was incubated with (1 U) micrococcal nuclease and 1 mM $CaCl_2$ at 37°C for 1 min. Reactions were stopped by adding EDTA to a final concentration of 5 mM on ice. Chromatin was prepared from nuclei disrupted by sonication at 4°C, then layering 20 μl of the suspension over a 100 μl pad of 80% glycerol. After centrifugation (10,000 rpm, 4°C, 15 min), the chromatin pellet was resuspended in the appropriate volume of TE and the DNA concentration was determined by fluorimetry.

Removal of histone H1

Histone H1 was removed from the chromatin preparations as previously described [59]. In brief, the chromatin solution was adjusted to 50 mM sodium phosphate (pH 7.0), 0.2 mM EDTA, and 100 mM NaCl and stirred in the presence of one-quarter of the volume of the ion exchange resin AG50W-X2 (Bio-Rod, USA) on ice for 90 min. The resin was pelleted at 500 × g for 5 min. After centrifugation, the supernatant containing H1-depleted chromatin was carefully collected for later analysis, and stored at –80°C for subsequent analysis.

Purification of histone proteins

Histone proteins were isolated from liver cell nuclei as described in details earlier [60]. All the following steps were performed at 4°C. Nuclear pellets prepared as described above were resuspended and then incubated in 0.2 M H_2SO_4 for 4 h prior to centrifugation (10,000 × g, 20 min). The supernatant containing acid-soluble proteins was collected and was incubated with 20% trichloroacetic acid overnight. After centrifugation (16,000 × g, 30 min), the pellets containing all histone proteins were washed once in ice-cold acetone containing 1% HCl and then washed once with ice-cold acetone. Pellets were vacuum-desiccated and stored at −80°C until further use. Components of histone proteins were resolved by SDS-PAGE using an 8–16% gradient gel, with subsequent Coomassie staining.

Electron microscopy

For analysis by electron microscopy, chromosomal samples were fixed at 4°C for at least 15 h by

adjusting the solutions in the corresponding buffers to 0.1% glutaraldehyde. For chromosome spreading, the fixed samples were diluted at room temperature with the corresponding fixation buffers to an A_{260} of 0.02–0.06, and BAC [61] was added from a stock solution in water (0.2 g/100 ml) to a concentration of 2×10^{-4}% ($\sim 7 \times 10^{-4}$ mM). After 30 min, droplets of 5 μl were applied to carbon-coated grids fixed on a sheet of Parafilm (American Can Co., Greenwich, Conn.). Adsorption of the chromatin fibers to the grids was allowed to take place for 5 min. The grids were washed with redistilled water for 10 min, dehydrated for 2–3 s in ethanol, and blotted dry on filter paper. For contrast enhancement, the grids were rotary-shadowed at an angle of 7° using carbon-platinum evaporated from an electron gun. Samples were examined in a Siemens electron microscope.101 at ×20,000. For the magnification calibration, a carbon grating replica grid from Balzers Union (Lichtenstein) was used [59].

Determination of the effect of p-Tau on DNA antioxidation

Copper, ascorbate, and 1,10-phenanthroline were premixed in 0.1 M NaOAc/HOAc (pH 5.2) buffer as described by Ma et al. [62]. Protein was premixed with DNA for at least 20 min in a NaOAc/HOAc buffer solution. Samples were incubated with phen-Cu/ascorbate at 37°C for 5 min. Afterwards, H_2O_2 was added to the solution to give a final volume of 100 μl. The chemiluminescence produced in the phen-Cu/H_2O_2/ascorbate system was immediately recorded with a computerized high sensitivity microplate luminometer (Type Centro XS³ LB 960, Berthold, manufactured at the Institute of Biophysics, China). The voltage on the photomultiplier was kept at 1000 V (**$p < 0.01$). A chemiluminescence profile of the DNA (1 μg vector Prk172 bearing *tau*$_{352}$)/protein (*p*-Tau, native tau, histone H1 and BSA) complex was recorded using thephen-Cu/H_2O_2/ascorbate system. The [DNA]/[protein] ratios were set as 0.5, 1, and 2. Formaldehyde was mixed with DNA at different concentrations (0.05, 0.1, 0.3 and 1 mM) and analyzed using the same system. The final concentrations for phenanthroline, $CuSO_4$, H_2O_2 and ascorbate were 3.5×10^{-4} M, 5×10^{-4} M, 0.5% and 3.5×10^{-4} M, respectively.

Data analysis

Data are shown as means ± standard error (S.E.M). Means of formaldehyde concentrations or blot densities among groups were compared by ANOVA followed by a *post-hoc* test. Statistical analyses were performed with Origin 5.0 and SPSS 16.0 [63].

RESULTS

As previously reported by Lu et al., formaldehyde induces the translocation of GSK-3β into the nucleus and promotes nuclear tau to be hyperphosphorylated in both N2a cells and C57BL/6 N mouse brain cells [30], also with an observation that tau disassociated from genomic DNA. Therefore, we first investigated whether the DNA is damaged following hyperphosphorylation of tau as a result of formaldehyde exposure of cultured cells.

In order to observe DNA damage inside the cell nucleus, we used a TUNEL assay to stain DNA in N2a cells treated with different concentrations of formaldehyde (Fig. 1). Cell nuclei were slightly stained in media containing 0.05 mM (Fig. 1b) and 0.1 mM formaldehyde (Fig. 1c), compared to a negative control lacking formaldehyde (Fig. 1a). DNA staining was more intense after formaldehyde treatment of increasing concentrations, using 0.3 mM (Fig. 1d) and 1.0 mM (Fig. 1e). In DNase I treated cells used as a positive control, intense nuclear staining was observed (Fig. 1f). CCK-8 results indicated that the cell viability of formaldehyde-treated cells decreased significantly (Fig. 1g). Similar results were observed in SH-SY5Y cells (Supplementary Fig. 2). These results suggest that the strands of the genomic DNA are presumably structurally compromised in the presence of formaldehyde, which likely results in a compromised DNA structure, and ultimately in reduced cell viability and cell death.

In addition, hyperphosphorylation of nuclear tau was also observed in N2a cell nuclei by immunostaining with anti-pT181, anti-pS396 and anti-tau (Tau5) antibodies (Supplementary Fig. 3). Importantly, in the presence of formaldehyde, the fluorescent signal for *p*-Tau did not overlap with the Hoechst 33258 staining for DNA. As indicated in our previous work [64], nuclear tau protein was hyperphosphorylated after 24 h formaldehyde incubation and both SH-SY5Y and N2a cell viabilities decrease by ∼50%. These results suggest that the interaction between tau and DNA is disturbed once the protein is phosphorylated.

Prior to investigating the effect of phosphorylation on the association of tau and DNA, we expressed and purified tau protein from *E. coli* as described previously [51]. Coomassie staining identified a single band on the SDS gel, verifying the purity of the expressed

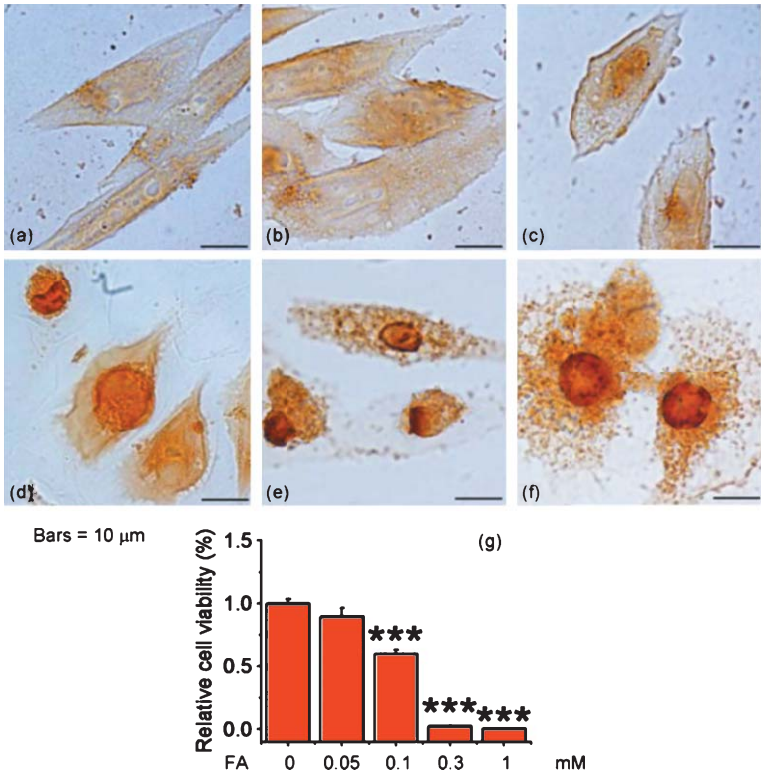

Fig. 1. Formaldehyde induces DNA damage in N2a cells. Different concentrations of formaldehyde (0.05 mM, 0.1 mM, 0.3 mM and 1.0 mM) were added to N2a cells for two days (b–e) and stained using a TUNEL assay. Microscopic images under bright field displayed TUNEL-stained DNA in N2a cells. Cells without formaldehyde (a) and cells treated with DNase I (f) were used as negative and positive control, respectively. Cell viability of formaldehyde-treated cells was measured using a CCK-8 assay (g). The control value was set as 1.0. All values were expressed as means ± S.E.M. ***$p < 0.001$, $n = 6$.

protein (Supplementary Fig. 1a). Phosphorylated tau was then prepared by incubating tau protein with GSK-3 overnight at 30°C. Phosphorylation of tau was confirmed by western blotting using residue-specific antibodies. As shown in Supplementary Fig. 1b, tau protein was phosphorylated at residues T181 and S396, with no background staining for phosphorylation in the negative control lacking GSK-3 treatment. In contrast, both samples were recognized by an anti-Tau antibody Tau5.

Next, we employed an EMSA test to investigate whether phosphorylation of tau interferes with its DNA binding. While distinct retardation was observed for the 26 bp dsDNA in the presence of native tau, no shift was detectable for *p*-Tau (Supplementary Fig. 4). In comparison, the controls used showed either distinct (histone H1) or little (BSA) retardation. Taken together, our results indicate that phosphorylation of tau markedly interferes with its binding ability to DNA.

Since phosphorylation drastically reduced the interaction between tau and DNA, we investigated if phosphorylation has an impact on the ability of tau to stabilize and protect the DNA. To this end, the hyperchromic effect, which is defined as an increase in absorption of ultraviolet light of DNA upon its denaturation, of tau and *p*-Tau during the transition of calf thymus dsDNA to single-stranded DNA (ssDNA) was studied under thermal condition. The observed kinetics of denaturation of the DNA followed a triphasic pattern: an initial slow phase, followed by a fast phase, and a final slow phase (Fig. 2a). The initial slow phase presumably corresponds to the relaxation phase, during which the DNA is unwinding. Our results show that non-phosphorylated, native tau slows down the rate of DNA denaturation when binding to DNA, which means DNA more strongly resists unwinding in the presence of tau binding. As shown in Fig. 2b, however, the time of maximal change in the absorbance of DNA with *p*-Tau shifted to 165 ± 20 s, significantly shorter ($p < 0.05$) than that of DNA bound by unphosphorylated tau (320 ± 31 s). In comparison, the absorbance maximum changes of DNA with BSA (116 ± 16 s)

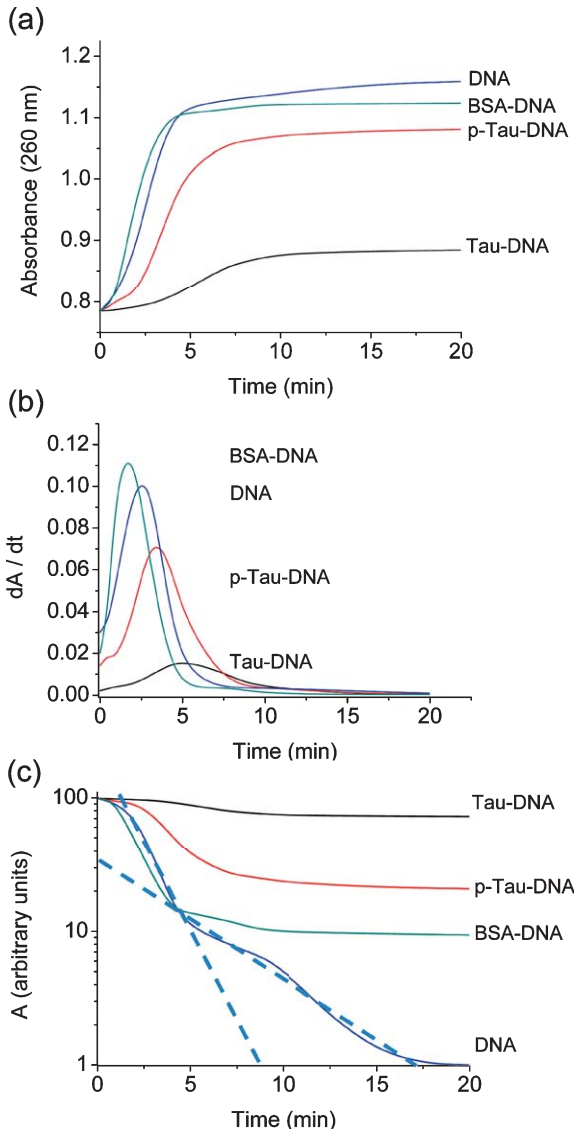

Fig. 2. Thermal denaturation of calf thymus DNA in the presence of phosphorylated tau. Calf thymus DNA was incubated with protein at 40 μg/ml in 10 mM Tris-EDTA buffer (pH 8.0) at 80°C, and absorbance was measured at 260 nm. The ratio of DNA to *p*-Tau ([DNA]/[protein]) was 1 (w/w). DNA alone, DNA plus native tau, or DNA plus BSA were used as controls (a). The same data were plotted as differentials (dA/dt) (where A and t represent the absorbance and time, respectively (b), or in semilogarithmic form, according to Tsou (c) [56].

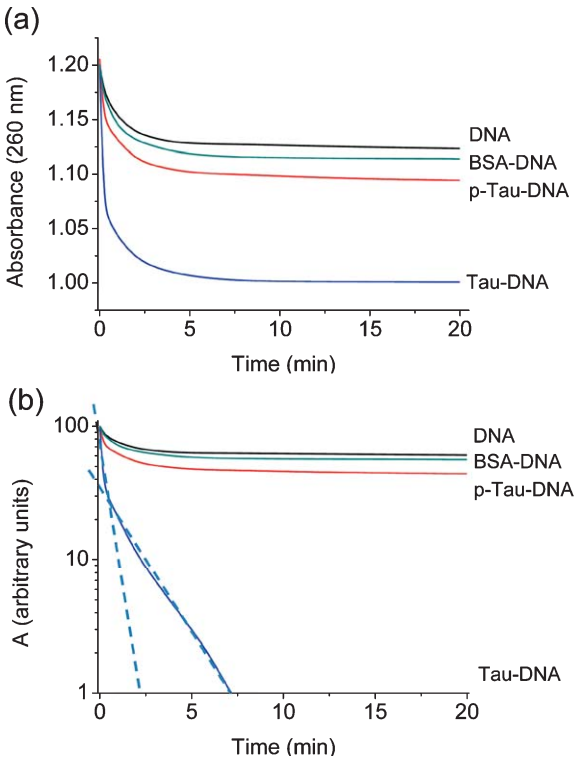

Fig. 3. Renaturation of calf thymus DNA in the presence of phosphorylated tau upon removal of thermal conditions. Conditions were as for Fig. 2, except that renaturation was measured at room temperature after boiling for 20 min at 100°C. DNA alone, DNA plus native tau, or DNA plus BSA were used as controls (a). Data were plotted in semi-logarithmic form according to Tsou (b) [56].

and DNA alone (143 ± 18 s) were significantly shorter. This suggests that the ability of tau protein to stabilize DNA during thermal denaturation is greatly reduced upon hyperphosphorylation.

To confirm that phosphorylation of tau disrupts its DNA binding ability, we next measured the changes in absorbance in a DNA hyperchromic reaction assay, and the first order rate constants were calculated according to Tsou (Fig. 2c) [56]. In the presence of *p*-Tau, the rate constant of the fast phase of DNA denaturation was about five-fold higher than that of unphosphorylated tau, and with the relaxation time being more than three-fold shorter (Table 1). The rate constant of the control samples containing DNA alone or DNA in the presence of BSA was approximately ten-fold larger than that of DNA with unphosphorylated tau. Given the distinctly faster hyperchromic process for the DNA/*p*-Tau complex, these data suggest that phosphorylation interferes with the ability of tau to delay the thermal denaturation of DNA.

To measure correctly the hyperchromic effect of tau during the transition of dsDNA to ssDNA, it is necessary to investigate whether the absorbance of tau interferes with that of DNA at 260 nm. We determined that the absorbance of tau between 240–300 nm was less than 0.05, probably due to the fact that tau does not contain any Trp residues. Thus, the observed absorbance of tau was considered to be below background signal [5].

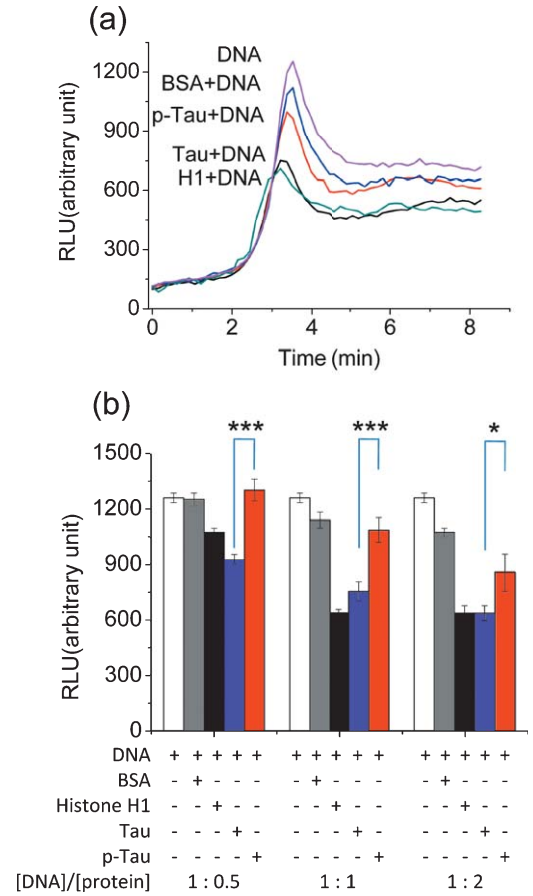

Fig. 4. Ability of tau to prevent peroxidation of DNA. To obtain a chemiluminescence data, DNA (1 μg of vector Prk172 bearing tau_{352}) was incubated with different proteins (*p*-Tau, native tau, BSA, and histone H1, [DNA]/[protein] = 1) in the phen-Cu/H_2O_2/ascorbate complex. One data point was recorded every 2 s, which represents the total intensity within this time interval. The concentrations of other reagents were phenanthroline (3.5×10^{-4} M), $CuSO_4$ (5×10^{-4} M), H_2O_2 (0.5%) and ascorbate (3.5×10^{-4} M) (a). Changes in the maximal chemiluminescence of DNA incubated with different concentrations of proteins in the phen-Cu/H_2O_2/ascorbate complex were as indicated (b). ***$p < 0.001$, $n = 3$.

To demonstrate if phosphorylation interferes with the actual binding of tau to DNA, we compared the effect of *p*-Tau on renaturation of thermally denatured DNA with that of native tau, upon instant exposure of the denatured DNA to room temperature. We found that renaturation of calf thymus DNA followed a rapid biphasic pattern, with an initial fast and a subsequent slow phase (Fig. 3a). The observed slow phase suggests that, following the formation of a double helix structure, the DNA is undergoing further folding into a structure of higher compaction. The rate of the fast phase of DNA refolding in the presence of tau was at least eight-fold higher than that of the control sample (Table 2). The rate of the slow phase step was of comparable magnitude, and about nine-fold higher than that of the control sample. Thus, unphosphorylated tau improved DNA refolding during renaturation following thermal denaturation, accelerating both the fast phase and the slow phase. The fact that tau could discriminate the double strands from single strand and then bind to DNA implied that the equilibrium between native and denatured DNA was progressively shifted towards the native form, a process induced by the presence of tau [5]. In contrast, *p*-Tau did not exhibit the effective acceleration observed for unphosphorylated tau at the fast and the slow phases of this assay (Fig. 3, Table 2). In conclusion, our results suggest that for tau to assist the refolding process of DNA upon renaturation after thermal denaturation, it must be present in its unphosphorylated form, since *p*-Tau exhibited a greatly diminished ability to do so.

After investigating the protective function of tau for DNA strand, we analyzed the relationship between tau and other biological factors known to be hazardous to the structure of DNA. The hydroxyl free radical, the

Table 1
First order rate constants of DNA denaturation in the presence of tau and *p*-Tau

	Relaxation time (s)	Fast rate constant (s^{-1})	Slow rate c onstant (s^{-1})
Tau-DNA	~200 ± 16	9.60 ± 1.21	2.28 ± 0.23
p-Tau-DNA	~60 ± 5.0	54.80 ± 4.32	7.68 ± 0.64
BSA-DNA	<10 ± 1.0	102.12 ± 11.22	13.71 ± 1.41
DNA	<10 ± 1.0	118.34 ± 12.45	31.92 ± 3.46

Cuvettes were incubated in an ultraviolet spectrophotometer, with a constant instrument temperature of 80°C. When sample was added into the cuvette, within 20 s the absorbance was measured for 20 min at 260 nm. Each data point represents three independent experiments. The ratio (w/w) of [DNA]/[protein] was equal to 1. All data were analyzed according to Tsou [54]. All kinetic rate constants are in $10^4 \times s^{-1}$.

Table 2
First-order rates of the decrease in absorbance of DNA at 260 nm upon incubation with tau and *p*-Tau

	Fast rate constant (s^{-1})	Slow rate constant (s^{-1})
Tau-DNA	384.87 ± 28.32	80.83 ± 7.69
p-Tau-DNA	95.95 ± 8.76	25.54 ± 2.21
BSA-DNA	61.40 ± 5.94	16.67 ± 1.45
DNA	51.21 ± 4.38	9.72 ± 1.01

Samples were incubated at 100°C for 20 min before annealing (renaturation) was initiated. The absorbance at 260 nm was detected within 20 s, following the addition of the sample into the cuvette at room temperature. The ratio (w/w) of [DNA]/[protein] was 1. All data were analyzed according to Tsou [54]. Kinetic rate constants (means ± S.D.) are presented as $10^4 \times s^{-1}$.

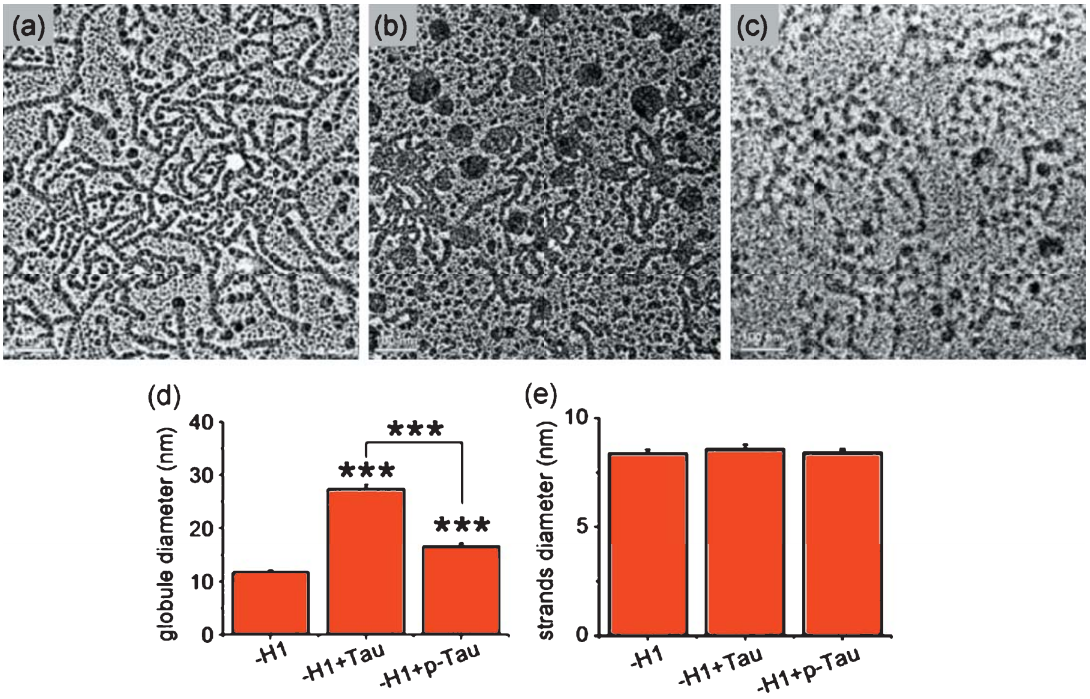

Fig. 5. Visualization of tau associated with DNA by electronic microscopy. Images represent DNA without histone H1 as control (a), DNA with unphosphorylated tau (b), DNA with *p*-Tau (c), a column plot to indicate the diameters of folded DNA chains (d), and the diameters of unfolded DNA chains (e). Bars = 100 nm, $***p < 0.001$, $n = 30$.

most noxious free radical amongst the ROS, is one of various factors resulting in DNA damage, and its presence in the nucleus can result in broken DNA strands [65]. Thus, we studied the ability of tau to protect DNA from structural impairment by hydroxyl free radicals *in vitro*. To this end, we employed a phen-copper complex method, where oxidative DNA damage was induced, with the resulting luminescence emission measured from the chemical reaction between DNA and hydroxyl free radicals, as described previously by Ma et al. [62]. As depicted in Fig. 4a, the luminescent intensity was markedly decreased upon addition of non-phosphorylated tau, an observation similar to the positive control sample containing histone H1. In contrast, luminescence emission was significantly higher when DNA was incubated with *p*-Tau instead. No protective effect was observed with BSA in lieu of tau (negative control). Furthermore, the luminescence intensities were significantly greater for the different ratios of [*p*-Tau]/[DNA], when compared to [Tau]/[DNA] (Fig. 4b, Supplementary Fig. 5). Thus, the DNA damage occurred mainly in the presence of phosphorylated tau, and phosphorylation prevented tau from protecting DNA under the attack of hydroxyl free radicals.

To rule out the possibility that DNA damage was directly caused by formaldehyde, the plasmid DNA was incubated with different concentrations of formaldehyde and then subjected to agarose gel electrophoresis. As shown in Supplementary Fig. 6a, DNA was not compromised by formaldehyde, as it was in the presence of DNase I. To confirm that formaldehyde does not directly break DNA strand, plasmid DNA treated with different concentrations of formaldehyde was added to the phen-copper complex (Supplementary Fig. 6b). The luminescence emission of DNA with formaldehyde (1.0 mM) was not significantly higher than that of DNA alone as control (Supplementary Fig. 6c). This suggests that formaldehyde does not directly contribute to the breakage of plasmid DNA.

Finally, to clarify why native tau, but not *p*-Tau, is capable of protecting DNA structure, we investigated the structures of both protein-DNA complexes. We isolated chromatin from rat liver, and removed histone H1 from the chromatin (Fig. 5a, Supplementary Fig. 7) as described by Thoma and colleagues [59]. In the presence of native tau, DNA converted to a folded structure (average diameter, 27.42 ± 0.73 nm) as shown in Fig. 5b and Table 3. Such conformation is likely to shield DNA double-strands from damage,

Table 3
Diameter of DNA globules and strands

	globule diameter (nm) Mean ± SE	Strands diameter (nm) Mean ± SE
DNA without H1	11.77 ± 0.37	8.37 ± 0.19
Tau23 + DNA	27.42 ± 0.73	8.57 ± 0.20
p-Tau + DNA	16.65 ± 0.51	8.42 ± 0.16

Images were taken by electron microscopy. 30 locations along the unfolded DNA chain were sampled randomly, and their vertical and horizontal widths were measured as globule and strand diameters, respectively.

by preventing an attack by free radicals. Addition of *p*-Tau, in contrast, did not result in a folded conformation of DNA (Fig. 5c). There was no significant difference in DNA strand diameter among the three groups. However, the globular diameter of DNA in the *p*-Tau group was significantly lower than that of the tau group (Fig. 5d,e and Table 3), indicating a smaller degree of DNA folding in the presence of *p*-Tau. This is presumably a result of a reduction in the binding ability of tau to DNA upon phosphorylation, therefore preventing the formation of Tau-DNA complexes.

DISCUSSION

Although much work on the correlation of tau hyperphosphorylation and cytoskeletal collapse has been carried out, the effect of hyperphosphorylation of tau protein on its interaction with nuclear DNA had not been studied in any detail. As shown here, phosphorylation of tau markedly interferes with its binding to and protecting of DNA from structural damage. In comparison, native tau is capable of inducing DNA into a folded structure, which possibly provides protection from attacks by intracellular ROS. These results suggest that a posttranslational modification like phosphorylation, can initiate dissociation of tau from DNA, resulting in greater instability of DNA and increased vulnerability to structural damage, alongside with its effect on microtubule disassembly, axonal transport impairment, and even cell death [15–17].

Our work provides evidence that tau cannot fulfill its function in protecting DNA once it becomes hyperphosphorylated. First, during thermal denaturation of DNA, *p*-Tau was unable to interfere with the transition of dsDNA to ssDNA. Second, *p*-Tau was also impaired in its function in accelerating renaturation of unfolded DNA (refolding). Third, the fluorescent signals of phosphorylated nuclear tau did not overlap with DNA staining with Hoechst 33258 in N2a cells in the presence of formaldehyde [64]. Fourth, in an EMSA assay, *p*-Tau only minimally reduced the mobility of DNA when compared with native tau. Fifth, when N2a cells were exposed to formaldehyde, DNA damage was observed in a TUNEL assay, correlated with the fact that formaldehyde can cause hyperphosphorylation of nuclear tau. Sixth, Sultan and colleagues have shown that nuclear tau protects DNA strand in heat-stressed neurons, demonstrating tau-mediated DNA protection in post-mitotic neurons [9]. Finally, upon phosphorylation of tau, DNA was not protected any more from structural impairment by hydroxyl radicals. Our experimental results suggest that upon phosphorylation, tau loses its protective function of maintaining the structure of nuclear DNA.

One possible explanation for the observed loss in binding ability of tau to DNA upon hyperphosphorylation is the drastic change in overall charge. This assumption is based on the following points: 1) Tau protein contains much more negative charges after being hyperphosphorylated, which interferes with its binding to the equally negatively charged DNA double strand; 2) As described in our previous work, when Lys is interacting with DNA bases by electrostatic interaction, the pK of its ε-amino group is 10.8 [9, 66]; 3) The interaction between tau and DNA is markedly reduced at pH higher than 12, indicating that the interaction depends on electrostatic forces; and 4) Modification of tau *in vitro* with formaldehyde results in reduced association of tau with DNA [40].

As described previously by Wei and colleagues [9], tau protein is able to bend DNA double strands upon association. This is due to the fact that both the microtubule-binding domain and the proline-rich domain of tau can interact simultaneously with the minor groove of DNA double-strands longer than 12 bp. This interaction resembles that of other sequence-nonspecific DNA-binding proteins such as high-mobility group proteins [67], which can bend DNA chain, with two or more of their protein domains interacting with the DNA double-strand at different regions of the minor groove. It is reasonable to suggest that association of tau protein with DNA can bend and fold DNA double-strands into a folded conformation.

Tau-induced folding of DNA may play a role in increasing its resistance to an attack by ROS, a viewpoint based on the following observations: 1) As described previously [9, 68], tau can induce a conformational change in DNA, with the more compact form displaying greater resistance to thermal denaturation; 2) Histone H1 is one major DNA-binding protein that mediates DNA protection. However, it displays typical folded conformations of DNA observed by atomic force microscope by Qu and coworkers [6]. In contrast,

BSA cannot protect DNA and did not show any folded conformations of DNA chain with the electron microscopy (Supplementary Fig. 8); 3) *p*-Tau exhibits weak protection of DNA *in vitro* either as less conformational change into a folded DNA structure was observed; and 4) As previously suggested, a folded conformation is not only able to shield DNA from the attack of ROS, but also from other incidents, such as chromosomal separation errors during mitosis [69], or enzymatic modification by DNA glycosylases [70].

Formaldehyde can react with DNA, resulting in induction of DNA chain crosslinking [71, 72]. As mentioned above, formaldehyde is able to induce tau hyperphosphorylation and DNA damage in N2a cells. DNA may undergo the loss of protection of tau because of tau hyperphosphorylation. The DNA damage possibly coincides with tau hyperphosphorylation, which in turn is caused by the formaldehyde treatment. Whether DNA crosslinking occurs under our experimental conditions needs further investigation. However, DNA strand breakage could not be detected after treatment with formaldehyde by luminescence assay as mentioned above. This indicates that the likely cause for DNA breakage is the loss of protection upon phosphorylation of tau.

Elevation of endogenous formaldehyde levels may be related to the pathogenic process in neurodegenerative diseases [73–75]. In one such example, namely age-related cognitive impairment, an increase in extracellular formaldehyde level was observed in the cerebrospinal fluid [76, 77]. AD is characterized by loss of neurons and synapses in the cerebral cortex and certain subcortical regions. As described previously, tau displays high DNA binding affinity, which is thought to be associated with protection of the DNA double strand. What is more, as shown here, hyperphosphorylation reduces the ability of tau in the protection of DNA in the presence of formaldehyde. Formaldehyde-induced tau hyperphosphorylation and DNA damage could present a putative mechanism behind the observed neuron loss in age-related cognitive impairment.

In summary, hyperphosphorylation of tau reduces its ability to prevent DNA from thermal denaturation; it loses the ability to accelerate DNA renaturation; it exhibits reduced functionality in protecting DNA from ROS attack; and it does not assist dsDNA from forming a folded structure. Therefore, hyperphosphorylation of tau is not only correlated with disassembly of the microtubule system, but it appears to be associated with the disassociation from and damage of DNA. Future investigation of the relationship between tau hyperphosphorylation and DNA damage may shed further light on the underlying molecular mechanisms resulting in tau-related neurodegenerative diseases.

ACKNOWLEDGMENTS

We thank Dr. Chan-Shuai Han for helpful comments in the experimental design and the entire He group for critical discussion of the manuscript. We also appreciate Dr. Goedert and Dr. Torsten Juelich for kindly providing the Prk172 vector and language editing, respectively. This project was supported by the 973-Project (2012CB911000; 2010CB912303), the Queensland-Chinese Academy of Sciences Biotechnology Fund (GJHZ1131) and the External Cooperation Program of BIC, Chinese Academy of Sciences (GJHZ201302).

Authors' disclosures available online (http://www.j-alz.com/disclosures/view.php?id=1867).

SUPPLEMENTARY MATERIAL

Supplementary figures are available in the electronic version of this article: http://dx.doi.org/10.3233/JAD-130602.

REFERENCES

[1] Stoothoff WH, Johnson GV (2005) Tau phosphorylation: Physiological and pathological consequences. *Biochim Biophys Acta* **1739**, 280-297.

[2] Weingarten MD, Lockwood AH, Hwo SY, Kirschner MW (1975) A protein factor essential for microtubule assembly. *Proc Natl Acad Sci U S A* **72**, 1858-1862.

[3] Drechsel DN, Hyman AA, Cobb MH, Kirschner MW (1992) Modulation of the dynamic instability of tubulin assembly by the microtubule-associated protein tau. *Mol Biol Cell* **3**, 1141-1154.

[4] Gotz J, Ittner LM, Kins S (2006) Do axonal defects in tau and amyloid precursor protein transgenic animals model axonopathy in Alzheimer's disease? *J Neurochem* **98**, 993-1006.

[5] Hua Q, He RQ (2003) Tau could protect DNA double helix structure. *Biochim Biophys Acta* **1645**, 205-211.

[6] Qu MH, Li H, Tian R, Nie CL, Liu Y, Han BS, He RQ (2004) Neuronal tau induces DNA conformational changes observed by atomic force microscopy. *Neuroreport* **15**, 2723-2727.

[7] Ugolini G, Cattaneo A, Novak M (1997) Co-localization of truncated tau and DNA fragmentation in Alzheimer's disease neurones. *Neuroreport* **8**, 3709-3712.

[8] Sultan A, Nesslany F, Violet M, Begard S, Loyens A, Talahari S, Mansuroglu Z, Marzin D, Sergeant N, Humez S, Colin M, Bonnefoy E, Buee L, Galas MC (2011) Nuclear tau, a key player in neuronal DNA protection. *J Biol Chem* **286**, 4566-4575.

[9] Wei Y, Qu MH, Wang XS, Chen L, Wang DL, Liu Y, Hua Q, He RQ (2008) Binding to the minor groove of the double-strand, tau protein prevents DNA from damage by peroxidation. *PLoS One* **3**, e2600.

[10] Buee L, Delacourte A (2006) [Tauopathy and Alzheimer disease: A full degenerating process]. *Psychol Neuropsychiatr Vieil* **4**, 261-273.
[11] Geschwind DH (2003) Tau phosphorylation, tangles, and neurodegeneration: The chicken or the egg? *Neuron* **40**, 457-460.
[12] Liu F, Grundke-Iqbal I, Iqbal K, Gong CX (2005) Contributions of protein phosphatases PP1, PP2A, PP2B and PP5 to the regulation of tau phosphorylation. *Eur J Neurosci* **22**, 1942-1950.
[13] Chen F, David D, Ferrari A, Gotz J (2004) Posttranslational modifications of tau - Role in human tauopathies and modeling in transgenic animals. *Curr Drug Targets* **5**, 503-515.
[14] Alonso A, Zaidi T, Novak M, Grundke-Iqbal I, Iqbal K (2001) Hyperphosphorylation induces self-assembly of tau into tangles of paired helical filaments/straight filaments. *Proc Natl Acad Sci U S A* **98**, 6923-6928.
[15] Feijoo C, Campbell DG, Jakes R, Goedert M, Cuenda A (2005) Evidence that phosphorylation of the microtubule-associated protein Tau by SAPK4/p38 delta at Thr50 promotes microtubule assembly. *J Cell Sci* **118**, 397-408.
[16] Terwel D, Muyllaert D, Dewachter I, Borghgraef P, Croes S, Devijver H, Van Leuven F (2008) Amyloid activates GSK-3beta to aggravate neuronal tauopathy in bigenic mice. *Am J Pathol* **172**, 786-798.
[17] Iqbal K, Alonso Adel C, Chen S, Chohan MO, El-Akkad E, Gong CX, Khatoon S, Li B, Liu F, Rahman A, Tanimukai H, Grundke-Iqbal I (2005) Tau pathology in Alzheimer disease and other tauopathies. *Biochim Biophys Acta* **1739**, 198-210.
[18] Gotz J, Gladbach A, Pennanen L, van Eersel J, Schild A, David D, Ittner LM (2010) Animal models reveal role for tau phosphorylation in human disease. *Biochim Biophys Acta* **1802**, 860-871.
[19] Alonso AC, Li B, Grundke-Iqbal I, Iqbal K (2008) Mechanism of tau-induced neurodegeneration in Alzheimer disease and related tauopathies. *Curr Alzheimer Res* **5**, 375-384.
[20] Goedert M, Jakes R, Spillantini MG, Hasegawa M, Smith MJ, Crowther RA (1996) Assembly of microtubule-associated protein tau into Alzheimer-like filaments induced by sulphated glycosaminoglycans. *Nature* **383**, 550-553.
[21] Hardy J (2006) A hundred years of Alzheimer's disease research. *Neuron* **52**, 3-13.
[22] Wu YH, Feenstra MGP, Zhou JN, Liu RY, Torano JS, Van Kan HJM, Fischer DF, Ravid R, Swaab DF (2003) Molecular changes underlying reduced pineal melatonin levels in Alzheimer disease: Alterations in preclinical and clinical stages. *J Clin Endocrinol Metab* **88**, 5898-5906.
[23] Binder LI, Guillozet-Bongaarts AL, Garcia-Sierra F, Berry RW (2005) Tau, tangles, and Alzheimer's disease. *Biochim Biophys Acta* **1739**, 216-223.
[24] Wang JZ, Tian Q (2012) Molecular mechanisms underlie Alzheimer-like tau hyperphosphorylation and neurodegeneration. *Prog Biochem Biophys* **39**, 771-777.
[25] Wei Y, Chen L, Chen J, Ge L, He RQ (2009) Rapid glycation with D-ribose induces globular amyloid-like aggregations of BSA with high cytotoxicity to SH-SY5Y cells. *BMC Cell Biol* **10**, 10.
[26] Hu JJ, Sun C, Lan L, Chen YW, Li DG (2010) Therapeutic effect of transplanting beta(2)m(−)/Thy1(+) bone marrow-derived hepatocyte stem cells transduced with lentiviral-mediated HGF gene into CCl(4)-injured rats. *J Gene Med* **12**, 244-254.
[27] Lan L, Chen YW, Sun C, Liu BW, Sun QL, Li DG (2009) Effect of interleukin 10 gene-modified bone marrow-derived liver stem cells transplantation on hepatic inflammatory response and liver regeneration in hepatic fibrosis rats. *Zhonghua Gan Zang Bing Za Zhi* **17**, 915-920.
[28] Langbaum JB, Fleisher AS, Chen K, Ayutyanont N, Lopera F, Quiroz YT, Caselli RJ, Tariot PN, Reiman EM (2013) Ushering in the study and treatment of preclinical Alzheimer disease. *Nat Rev Neurol* **9**, 371-381.
[29] He RQ (2012) The research window of Alzheimer's disease should be brought forward. *Prog Biochem Biophys* **39**, 692-697.
[30] Lu J, Miao J, Su T, Liu Y, He R (2013) Formaldehyde induces hyperphosphorylation and polymerization of Tau protein both *in vitro* and *in vivo*. *Biochim Biophys Acta* **1830**, 4102-4116.
[31] Elyaman W, Terro F, Wong NS, Hugon J (2002) *In vivo* activation and nuclear translocation of phosphorylated glycogen synthase kinase-3 beta in neuronal apoptosis: Links to tau phosphorylation. *Eur J Neurosci* **15**, 651-660.
[32] Elyaman W, Yardin C, Hugon J (2002) Involvement of glycogen synthase kinase-3 beta and tau phosphorylation in neuronal Golgi disassembly. *J Neurochem* **81**, 870-880.
[33] Noble W, Planel E, Zehr C, Olm V, Meyerson J, Suleman F, Gaynor K, Wang L, LaFrancois J, Feinstein B, Burns M, Krishnamurthy P, Wen Y, Bhat R, Lewis J, Dickson D, Duff K (2005) Inhibition of glycogen synthase kinase-3 by lithium correlates with reduced tauopathy and degeneration *in vivo*. *Proc Natl Acad Sci U S A* **102**, 6990-6995.
[34] Gao X, Joselin AP, Wang L, Kar A, Ray P, Bateman A, Goate AM, Wu JY (2010) Progranulin promotes neurite outgrowth and neuronal differentiation by regulating GSK-3 beta. *Protein Cell* **1**, 552-562.
[35] He RQ, Lu J, Mia JY (2010) Formaldehyde stress. *Sci China Life Sci* **53**, 1399-1404.
[36] Tong ZQ, Zhang JL, Luo WH, Wang WS, Li FX, Li H, Luo HJ, Lu J, Zhou JN, Wan Y, He RQ (2011) Urine formaldehyde level is inversely correlated to mini mental state examination scores in senile dementia. *Neurobiol Aging* **32**, 31-41.
[37] Nie CL, Zhang W, Zhang D, He RQ (2005) Changes in conformation of human neuronal tau during denaturation in formaldehyde solution. *Protein Pept Lett* **12**, 75-78.
[38] Nie CL, Wei Y, Chen XY, Liu YY, Dui W, Liu Y, Davies MC, Tendler SJB, He RG (2007) Formaldehyde at low concentration induces protein tau into globular amyloid-like aggregates *in vitro* and *in vivo*. *PLoS One* **2**, e629.
[39] Nie CL, Wang XS, Liu Y, Perrett S, He RQ (2007) Amyloid-like aggregates of neuronal tau induced by formaldehyde promote apoptosis of neuronal cells. *BMC Neurosci* **8**, 9.
[40] Hua Q, He RQ (2002) Effect of phosphorylation and aggregation on tau binding to DNA. *Protein Pept Lett* **9**, 349-357.
[41] Tong Z, Han C, Luo W, Wang X, Li H, Luo H, Zhou J, Qi J, He R (2012) Accumulated hippocampal formaldehyde induces age-dependent memory decline. *Age (Dordr)* **35**, 583-596.
[42] Gong CX, Liu F, Grundke-Iqbal I, Iqbal K (2005) Post-translational modifications of tau protein in Alzheimer's disease. *J Neural Transm* **112**, 813-838.
[43] Li T, Paudel HK (2006) Glycogen synthase kinase 3 beta phosphorylates Alzheimer's disease-specific Ser396 of microtubule-associated protein tau by a sequential mechanism. *Biochemistry* **45**, 3125-3133.
[44] Liu F, Iqbal K, Grundke-Iqbal I, Rossie S, Gong CX (2005) Dephosphorylation of tau by protein phosphatase 5: Impairment in Alzheimer's disease. *J Biol Chem* **280**, 1790-1796.
[45] Blennow K (2005) CSF biomarkers for Alzheimer's disease: Use in early diagnosis and evaluation of drug treatment. *Expert Rev Mol Diagn* **5**, 661-672.
[46] Olsson A, Vanderstichele H, Andreasen N, De Meyer G, Wallin A, Holmberg B, Rosengren L, Vanmechelen E,

Blennow K (2005) Simultaneous measurement of beta-amyloid(1-42), total tau, and phosphorylated tau (Thr(181)) in cerebrospinal fluid by the xMAP technology. *Clin Chem* **51**, 336-345.

[47] De Meyer G, Shapiro F, Vanderstichele H, Vanmechelen E, Engelborghs S, De Deyn PP, Coart E, Hansson O, Minthon L, Zetterberg H, Blennow K, Shaw L, Trojanowski JQ, Initi AsDN (2010) Diagnosis-independent Alzheimer disease biomarker signature in cognitively normal elderly people. *Arch Neurol* **67**, 949-956.

[48] Abraha A, Ghoshal N, Gamblin TC, Cryns V, Berry RW, Kuret J, Binder LI (2000) C-terminal inhibition of tau assembly *in vitro* and in Alzheimer's disease. *J Cell Sci* **113**, 3737-3745.

[49] Michel G, Mercken M, Murayama M, Noguchi K, Ishiguro K, Imahori K, Takashima A (1998) Characterization of tau phosphorylation in glycogen synthase kinase-3 beta and cyclin dependent kinase-5 activator (p23) transfected cells. *Biochim Biophys Acta* **1380**, 177-182.

[50] Li P, He X, Gerrero MR, Mok M, Aggarwal A, Rosenfeld MG (1993) Spacing and orientation of bipartite DNA-binding motifs as potential functional determinants for Pou domain factors. *Genes Dev* **7**, 2483-2496.

[51] Hua Q, He RQ, Haque N, Qu MH, Alonso AD, Grundke-Iqbal I, Iqbal K (2003) Microtubule associated protein tau binds to double-stranded but not single-stranded DNA. *Cell Mol Life Sci* **60**, 413-421.

[52] Petro KA, Schengrund CL (2009) Membrane raft disruption promotes axonogenesis in N2a neuroblastoma cells. *Neurochem Res* **34**, 29-37.

[53] Ikonen M, Liu BR, Hashimoto Y, Ma LQ, Lee KW, Niikura T, Nishimoto I, Cohen P (2003) Interaction between the Alzheimer's survival peptide humanin and insulin-like growth factor-binding protein-3 regulates cell survival and apoptosis. *Proc Natl Acad Sci U S A* **100**, 13042-13047.

[54] Misawa A, Inoue J, Sugino Y, Hosoi H, Sugimoto T, Hosoda F, Ohki N, Imoto I, Inazawa J (2005) Methylation-associated silencing of the nuclear receptor 1I2 gene in advanced-type neuroblastomas, identified by bacterial artificial chromosome array-based methylated CpG island amplification. *Cancer Res* **65**, 10233-10242.

[55] Linask KK, Han MD, Cai DH, Brauer PR, Maisastry SM (2005) Cardiac morphogenesis: Matrix metalloproteinase coordination of cellular mechanisms underlying heart tube formation and directionality of looping. *Dev Dyn* **233**, 739-753.

[56] Xu GJ, Tsou CL (1964) Kinetics of effect of inhibitors on systems involving 2 enzyme-substrate intermediates. *Sci Sin* **13**, 269-277.

[57] Tan GS, Garchow BG, Liu XH, Yeung J, Morris JP, Cuellar TL, McManus MT, Kiriakidou M (2009) Expanded RNA-binding activities of mammalian Argonaute 2. *Nucleic Acids Res* **37**, 7533-7545.

[58] Noll M, Thomas JO, Kornberg RD (1975) Preparation of native chromatin and damage caused by shearing. *Science* **187**, 1203-1206.

[59] Thoma F, Koller T, Klug A (1979) Involvement of histone H1 in the organization of the nucleosome and of the salt-dependent superstructures of chromatin. *J Cell Biol* **83**, 403-427.

[60] Dedon PC, Soults JA, Allis CD, Gorovsky MA (1991) Formaldehyde cross-linking and immunoprecipitation demonstrate developmental-changes in H1-association with transcriptionally active genes. *Mol Cell Biol* **11**, 1729-1733.

[61] Vollenweider HJ, Sogo JM, Koller T (1975) A routine method for protein-free spreading of double- and single-stranded nucleic acid molecules. *Proc Natl Acad Sci U S A* **72**, 83-87.

[62] Ma WJ, Cao EH, Zhang J, Qin JF (1998) Phenanthroline-Cu complex-mediated chemiluminescence of DNA and its potential use in antioxidation evaluation. *J Photochem Photobiol B* **44**, 63-68.

[63] Xu YJ, Qiang M, Zhang JL, Liu Y, He RQ (2012) Reactive carbonyl compounds (RCCs) cause aggregation and dysfunction of fibrinogen. *Protein Cell* **3**, 627-640.

[64] Lu J, Miao JY, Pan R, He RQ (2011) Formaldehyde-mediated hyperphosphorylation disturbs the interaction between tau protein and DNA. *Prog Biochem Biophys* **38**, 1113-1120.

[65] Travers AA, Ner SS, Churchill MEA (1994) DNA chaperones - a solution to a persistence problem. *Cell* **77**, 167-169.

[66] Jensen DE, Vonhippel PH (1976) DNA melting proteins 1. Effects of bovine pancreatic ribonuclease binding on conformation and stability of DNA. *J Biol Chem* **251**, 7198-7214.

[67] Thomas JO, Travers AA (2001) HMG1 and 2, and related 'architectural' DNA-binding proteins. *Trends Biochem Sci* **26**, 167-174.

[68] Alonso AD, Zaidi T, Novak M, Barra HS, Grundke-Iqbal I, Iqbal K (2001) Interaction of tau isoforms with Alzheimer's disease abnormally hyperphosphorylated tau and *in vitro* phosphorylation into the disease-like protein. *J Biol Chem* **276**, 37967-37973.

[69] Ganem NJ, Pellman D (2012) Linking abnormal mitosis to the acquisition of DNA damage. *J Cell Biol* **199**, 871-881.

[70] Brooks SC, Adhikary S, Rubinson EH, Eichman BF (2013) Recent advances in the structural mechanisms of DNA glycosylases. *Biochim Biophys Acta* **1834**, 247-271.

[71] Kurdistani SK, Grunstein M (2003) *In vivo* protein-protein and protein-DNA crosslinking for genomewide binding microarray. *Methods* **31**, 90-95.

[72] Toth J, Biggin MD (2000) The specificity of protein-DNA crosslinking by formaldehyde: *In vitro* and in drosophila embryos. *Nucleic Acids Res* **28**, e4.

[73] Pitten FA, Kramer A, Herrmann K, Bremer I, Koch S (2000) Formaldehyde neurotoxicity in animal experiments. *Pathol Res Pract* **196**, 193-198.

[74] Kilburn KH, Warshaw R, Thornton JC (1987) formaldehyde impairs memory, equilibrium, and dexterity in histology technicians - effects which persist for days after exposure. *Arch Environ Health* **42**, 117-120.

[75] Perna RB, Bordini EJ, Deinzer-Lifrak M (2001) A case of claimed persistent neuropsychological sequelae of chronic formaldehyde exposure - Clinical, psychometric, and functional findings. *Arch Clin Neuropsychol* **16**, 33-44.

[76] Kuhla B, Luth HJ, Haferburg D, Boeck K, Arendt T, Munch G (2005) Methylglyoxal, glyoxal, and their detoxification in Alzheimer's disease. *Ann N Y Acad Sci* **1043**, 211-216.

[77] Ono K, Noguchi M, Matsumoto Y, Yanase D, Iwasa K, Naiki H, Yamada M (2005) Cerebrospinal fluid of Alzheimer patients promotes beta-amyloid fibril formation *in vitro*. *Neurobiol Dis* **20**, 233-240.